Effect of adsorbed polyelectrolytes on the interactions and elasticity of charged surfactant bilayers

Santosh Prasad Gupta[1]**, Meera Thomas, Anindya Chowdhury and V A Raghunathan**[2]

Raman Research Institute, Bangalore-560080, India

E-mail: varaghu@rri.res.in

CrossMark

Abstract

We present studies on the structure of complexes of the cationic, bilayer-forming surfactant, didodecyldimethylammonium bromide (DDAB), and the anionic polyelectrolyte sodium polyacrylate (PAANa). In the presence of uncomplexed polyelectrolyte in the coexisting aqueous solution, these complexes are found to exhibit a swelling transition followed by a deswelling transition on increasing the salt concentration. Lamellar structures with low periodicities occur at both low and high salt concentrations, which are stabilized by polymer bridging and van der Waals attraction, respectively. The swollen complex found at intermediate salt concentrations forms the sponge phase. Our results reveal that polyelectrolyte adsorption on bilayers has a profound effect on inter-bilayer interactions. The polymer-induced interaction changes from being attractive to repulsive as the surface coverage increases on increasing the salt concentration. Our results also confirm that polymer adsorption alters the elastic moduli of the bilayer, in agreement with earlier theoretical predictions.

Keywords: surfactant—polyelectrolyte complex, small angle x-ray scattering, swelling transition

S Supplementary material for this article is available online

(Some figures may appear in colour only in the online journal)

1. Introduction

Ionic amphiphiles, that self-assemble into bilayers, form a highly swollen lamellar phase in aqueous solutions, as a result of long-range electrostatic inter-bilayer repulsion [1–3]. Addition of an oppositely charged polyelectrolyte to the solution has a very pronounced effect on the inter-bilayer interactions, which depends sensitively on the salt concentration (c_s) in the solution [4, 5]. At low c_s the polyelectrolyte forms a heterogeneous adsorption layer on the bilayer surface, due to the electrostatic repulsion between the chains, as has been observed in the case of polyelectrolyte adsorption on oppositely charged rigid surfaces [6]. The presence of a patchy adsorption layer leads to the creation of polymer bridges between adjacent bilayer surfaces, resulting in an effective inter-bilayer attraction [4, 7]. As a consequence, a compact surfactant-polyelectrolyte complex precipitates out of the solution, in which a thin polyelectrolyte layer is sandwiched between successive bilayers [8]. The lamellar periodicity of this complex is only slightly higher than the bilayer thickness. On increasing c_s a homogeneous adsorption layer is formed on the bilayer surface due to the screening of inter-chain repulsion [4, 6, 9]. Bridging of neighboring bilayers is no longer possible [10] and the polyelectrolyte covered bilayers form a swollen complex, stabilized either by steric repulsion [11] between the adsorbed chains on adjacent bilayers or by

[1] Present address: Department of Physics, Patna University, Patna 800005, India
[2] Author to whom any correspondence should be addressed.

undulation repulsion [12], if the bilayer bending rigidity, κ, is sufficiently low [5]. At high c_s the polyelectrolyte desorbs from the bilayer surface. Since the electrostatic inter-bilayer repulsion is highly screened, van der Waals attraction dominates and the bilayers again form a lamellar phase with a very low periodicity, but with no polyelectrolyte in the intervening aqueous layer between the bilayers. Such salt-induced swelling and de-swelling transitions have been recently reported by us in complexes of the ionic surfactant didodecyldimethylammonium chloride (DDAC) and sodium salt of poly-acrylic acid (PAANa) [5].

Elasticity of a bilayer is described in terms of two moduli; the bending rigidity modulus κ and the Gaussian rigidity modulus $\bar{\kappa}$, which are associated with the mean and Gaussian curvatures of the surface, respectively [13, 14]. Stability requires κ to be positive, whereas there is no such restriction on the sign of $\bar{\kappa}$. Polymer adsorption on a bilayer has been predicted to alter both κ and $\bar{\kappa}$ [15, 16]. κ is expected to decrease, whereas $\bar{\kappa}$ is expected to increase in the presence of an adsorption layer. The DDAC-water system forms a swollen L_α phase when the electrostatic repulsion between the bilayers is screened by the addition of NaCl [5]. The lamellar periodicity of this phase is determined by undulation repulsion between the bilayers, which depends on κ [12, 17]. If the swollen DDAC-PAANa complex is also stabilized by undulation repulsion between the bilayers, it should in principle be possible to ascertain the effect of polymer adsorption on κ by comparing the maximal lamellar periodicities of the swollen complex and the DDAC-water-NaCl system. But it was not possible to address this issue unequivocally in [5], since the lamellar periodicity of the swollen complex showed a large spread, presumably as a result of the extremely slow equilibration due to the irreversible nature of the adsorption process [18].

Here we present studies on complexes of the ionic surfactant didodecyldimethylammonium bromide (DDAB) and PAANa. This system also exhibits the swelling and deswelling transitions observed earlier in DDAC-PAANa complexes. However, instead of forming a lamellar phase, the swollen complexes in the present system exhibits the sponge phase. The lamellar to sponge transition of bilayers is known to occur when $\bar{\kappa}$ increases and becomes weakly negative [19–22]. Therefore, the present results confirm that binding of PAANa to DDAB bilayers leads to an increase in $\bar{\kappa}$, in agreement with theoretical predictions. Formation of the sponge phase in DDAB-PAANa complexes, but not in DDAC-PAANa complexes, can be understood in terms of differences in the phase behaviour of aqueous solutions of these two surfactants, which suggest that DDAB bilayers have a higher $\bar{\kappa}$ compared to DDAC bilayers. Hence it should be easier to drive DDAB bilayers into the sponge phase than DDAC bilayers, in agreement with our observations.

2. Materials and methods

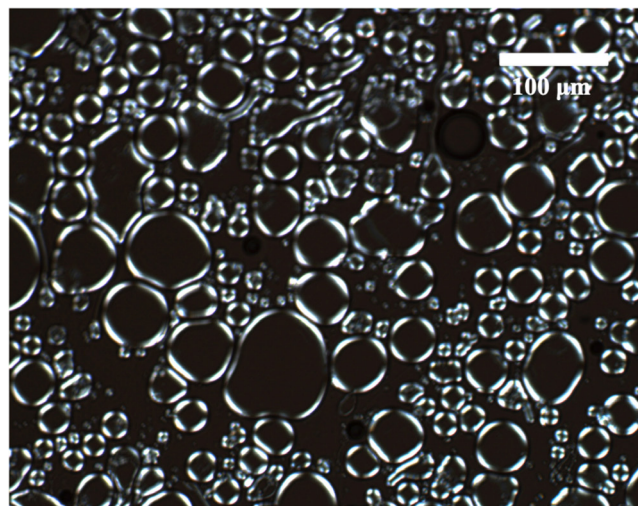DDAB, PAANa ($M_w = 2100$, 5100, 8000 and 15 000) and NaBr were purchased from Sigma-Aldrich and were used

Figure 1. POM textures of the L_α phase of DDAB-PAANa2100 complexes at $R = 14$, $\phi = 20$ and $T = 30\,°C$.

without further purification. Samples were prepared over a wide range of ϕ_s at a few values of R, ϕ_s being the combined weight percentage of DDAB and PAANa, and R the polyelectrolyte to surfactant weight ratio. Values of R chosen were much above the isoelectric point of the system ($R_{iso} = 0.2$), so that the coexisting aqueous solution in all cases contained uncomplexed polyelectrolyte. Ranges of ϕ_s and R were chosen in order to obtain all possible structures of the complexes. No additional structures are observed beyond the ranges used. Samples were prepared in Millipore water and were kept at 40 °C for about a month for equilibration.

Complexes were studied using polarizing optical microscopy (POM), small–angle x-ray scattering (SAXS) and cryogenic-scanning electron microscopy (cryo-SEM). Experimental details are presented in [5]. In addition, the composition of some of the complexes was probed using thermogravimetric analysis (TGA) and elemental analysis.

3. Results

At $R = 14$, DDAB-PAANa2100 complexes form a whitish precipitate for $\phi_s = 15$ and 20. The complex swells rather abruptly on increasing ϕ_s to 23, producing a well-separated layer on top of an aqueous solution. With further increase in ϕ_s the volume fraction of the complex decreases gradually. A whitish precipitate is again observed for $\phi_s > 65$. Viscosity of the coexisting aqueous solution is observed to increase with increasing ϕ_s.

Complexes formed at $\phi_s = 15$ and 20 are birefringent and exhibit Maltese cross and oily streak textures under POM, indicating their lamellar structure (figure 1). Swollen complexes found at higher values of ϕ_s are optically isotropic.

Cryo-SEM experiments have been carried out on the birefringent and isotropic complexes. A layered morphology is observed in the micrographs of the birefringent complexes (figure 2(a)). These micrographs show multilamellar vesicles of different sizes, further affirming the lamellar structure of
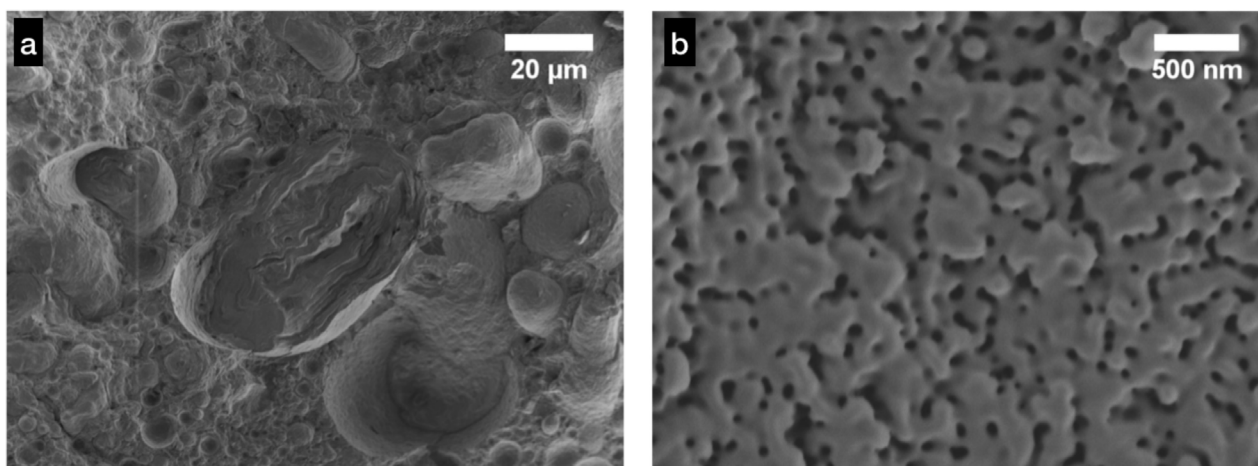
Figure 2. Cryo-SEM micrographs of DDAB-PAANa2100 complexes. (a) L_α phase at $R = 5$, $\phi_s = 20$. (b) L_3 phase at $R = 14$, $\phi_s = 50$.

these complexes. Such features are absent in the micrographs of the isotropic complexes. Instead, they show a convoluted structure, similar to that reported from the sponge (L_3) phase of surfactant systems (figure 2(b)) [23].

SAXS patterns of the complexes at $\phi_s = 15$ and 20 show two peaks in the small angle region, with the corresponding values of the magnitude of the scattering vector (q) in the ratio 1:2 (figure 3(a)). No sharp peaks are observed in the wide angle region for any of the complexes studied here. Hence it can be concluded that these complexes form a fluid lamellar (L_α) phase. Lamellar periodicity (d) is found to be about 3.5 nm. Diffraction data of these complexes were analyzed using the procedure described in [24], as outlined in supplementary material (stacks.iop.org/JPhysCM/32/194004/mmedia). Values of the model parameters obtained from the fits are given in table 1. Values of the bilayer thickness ($d_b = 2\,z_h$) obtained are in excellent agreement with the value of 2.2 nm reported in the literature for DDAB bilayers [2]. Further, as expected, the thickness of the water layer ($d_w = d - d_b$) separating the bilayers is only around 1 nm in this collapsed lamellar complex.

SAXS patterns of the optically isotropic swollen complex at $\phi_s = 23$ do not contain any sharp peaks. Similar patterns are also observed at $\phi_s = 26$, 30 and 35. However, at $\phi_s = 40$, the SAXS pattern has a very broad peak at very low q (figure 3(b)). SAXS data of the isotropic complexes were fitted to a model of the sponge (L_3) phase described in the literature [25], as outlined in supplementary material. Values of the model parameters obtained from the fit are given in table 2. At $\phi_s = 40$ the average cell–cell distance (L) of the L_3 phase, which corresponds to the position of the broad peak, is about 30 nm at 30 °C. Values of the cell–cell correlation length obtained are almost an order of magnitude smaller than those reported in the literature [25], indicating a large spread in the average cell–cell distance L. This can account for the small discrepancies between the observed and calculated intensity values at low q apparent in figure 3(b). An analogous situation was found in the case of DDAC-PAANa complexes, where the periodicity of the swollen lamellar phase was observed to have a large spread, leading to a substantial increase in the peak
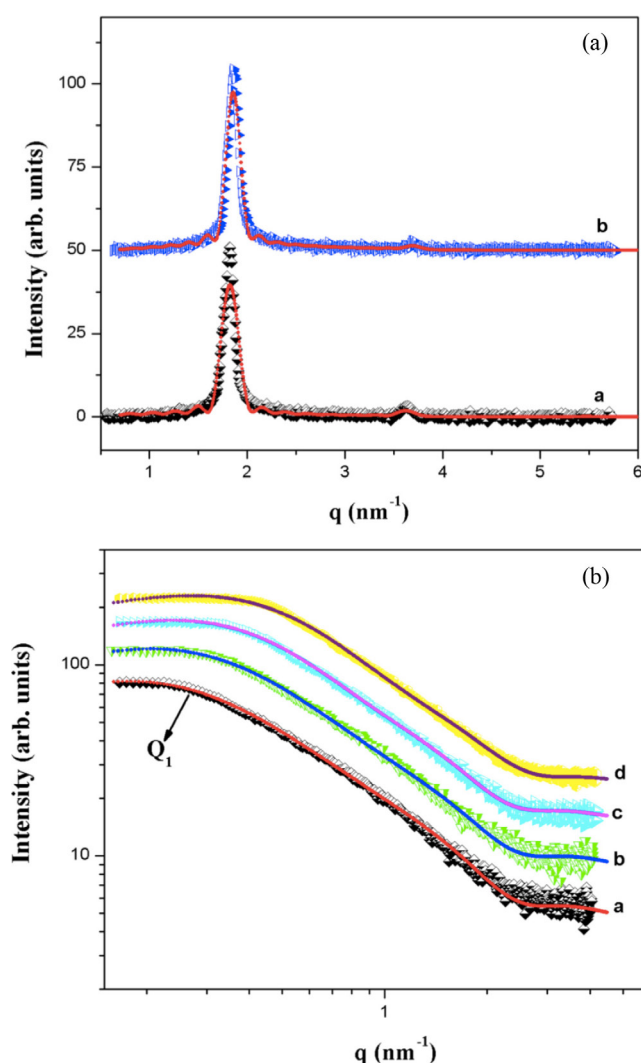

Figure 3. SAXS patterns of DDAB-PAANa2100 complexes at $R = 14$. (a) L_α phase at $\phi_s = 20$, $T = 30$ °C and 80 °C (curves (a) and (b), respectively). (b) L_3 phase at $\phi_s = 40$ and $T = 30$ °C, 40 °C, 50 °C and 60 °C (curves (a) to (d), respectively). Solid lines are fits to models for scattering from the L_α and L_3 phases referred to in the text. Q_1 indicates the position of the broad correlation peak in the L_3 phase.

Table 1. Values of model parameters obtained from fitting the diffraction data from DDAB-PAANa2100 complexes at $R = 14$ and $\phi_s = 15$ to the expression for scattering from the lamellar (L_α) phase given in [24]. σ_h and σ_c are the widths of the two Gaussian functions representing the electron densities of the headgroup region and bilayer mid-plane, respectively. ρ_h and ρ_c are the amplitudes of these two Gaussians. $2z_h$ is the separation between the electron density peaks corresponding to the two headgroup regions of a bilayer. η is the Caillé parameter and N the number of correlated bilayers.

T (°C)	30	80
σ_h (nm)	0.28 ± 0.02	0.28 ± 0.02
σ_c (nm)	0.46 ± 0.02	0.46 ± 0.02
ρ_c/ρ_h	-1.29 ± 0.08	-1.29 ± 0.08
z_h (nm)	1.10 ± 0.03	1.07 ± 0.03
η	0.039 ± 0.002	0.037 ± 0.002
N	10 ± 1	11 ± 1

Table 2. Values of the model parameters obtained from fitting the diffraction data from DDAB-PAANa2100 complexes at $R = 14$ and $\phi_s = 40$ to the model for scattering from the sponge (L_3) phase given in [25]. L is the average cell–cell distance. ξ_2 is the cell–cell correlation length. σ and w are the average radius and thickness of the bilayer discoids, respectively.

T (°C)	L (nm)	ξ_2 (nm)	σ (nm)	w (nm)
30	29.92	0.53	7.52	2.22
40	26.18	0.56	6.35	2.23
50	20.67	0.85	4.94	2.27
60	17.45	0.75	3.95	2.01

width [5]. L and the average radius of bilayer discoid (σ) are found to decrease on heating, indicating a gradual deswelling with increasing temperature. It is not clear if this results from changes in the bilayer properties with temperature or if changes in the polyelectrolyte adsorption layer play a role. SAXS patterns at $\phi_s = 30$ and $T = 30\,°C$ can also be fitted to this model. However, the value of L is too large to be accessed by our SAXS instrument. Thickness of the bilayer patches obtained from the model is about 2 nm, which is very close to the value of the bilayer thickness in the L_α phase (table 1).

POM images of the precipitate formed at $\phi_s = 70$ show a Maltese cross texture typical of a dispersion of multilamelar vesicles (figure 4). Its SAXS patterns indicate a periodicity of about 2.9 nm, which is slightly lower than that of the collapsed lamellar complex found at low values of ϕ_s (figure 5). The characteristic length of the complexes as a function of ϕ_s is given in figure 6, which shows clearly the swelling and deswelling transitions occurring at $\phi_s \approx 20$ and 65, respectively.

Phase behaviour of the complexes at lower values of R is qualitatively similar to that observed at $R = 14$ (figure 7). The L_α phase is stable over a wider range of water content for lower values of R and the L_α-L_3 boundary shifts to higher values of ϕ_s as R is reduced. Further, the L_3 phase exists over a wider range of ϕ_s at higher values of R. A second collapsed lamellar phase is formed at all values of R for $\phi_s > 65$, which is not indicated in figure 7.

To understand the effect of molecular weight of the polyelectrolyte on the swelling behaviour, complexes of DDAB
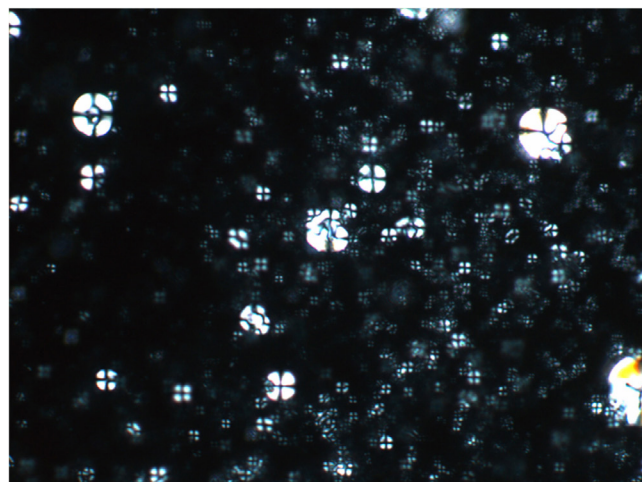

Figure 4. POM images of the second collapsed L_α phase at $R = 14$ and $\phi_s = 70$, showing a dispersion of multilamellar vesicles.
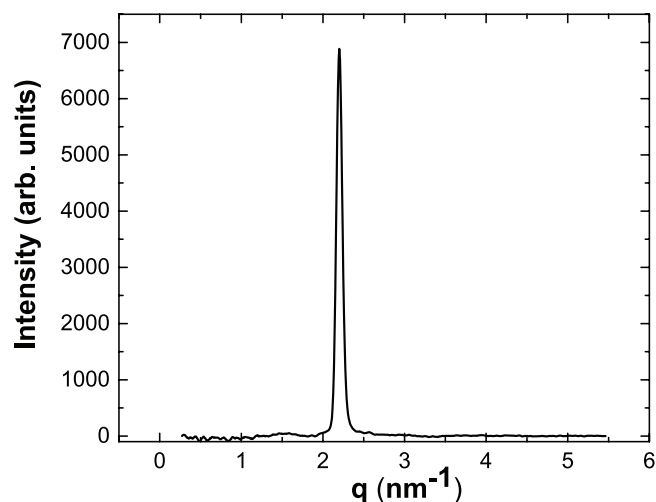

Figure 5. SAXS pattern of the second collapsed L_α phase at $R = 14$ and $\phi_s = 70$.

with PAANa of molecular weights 5100, 8000 and 15 000 were also studied. Phase behaviour of DDAB-PAANa5100 is found to be very similar to that of DDAB-PAANa2100. On the other hand, DDAB-PAANa8000 and DDAB-PAANa15000 do not exhibit the swelling behavior and they form a lamellar phase of very low periodicity for all values of ϕ_s. However, the lamellar periodicity shows a non-monotonic dependence on ϕ_s, with a maximum at $\phi_s \sim 30$ (figure 8).

As in the case of DDAC-PAANa complexes [5], it is possible to drive the swelling and deswelling transitions by increasing the salt (NaBr) concentration in the solution at $R = 14$, $\phi_s = 20$. The swollen complexes are again found to exhibit the L_3 phase. TGA of the two lamellar complexes formed at low and high c_s were carried out to determine their composition (figure 9). TGA curves of the surfactant and polymer solutions were also collected for reference. Both of them show a step at around 100 °C corresponding to the loss of water. Loss of the surfactant occurs at around 200 °C, whereas that of the polymer occurs at around 400 °C. The large difference in the degradation temperatures of these two
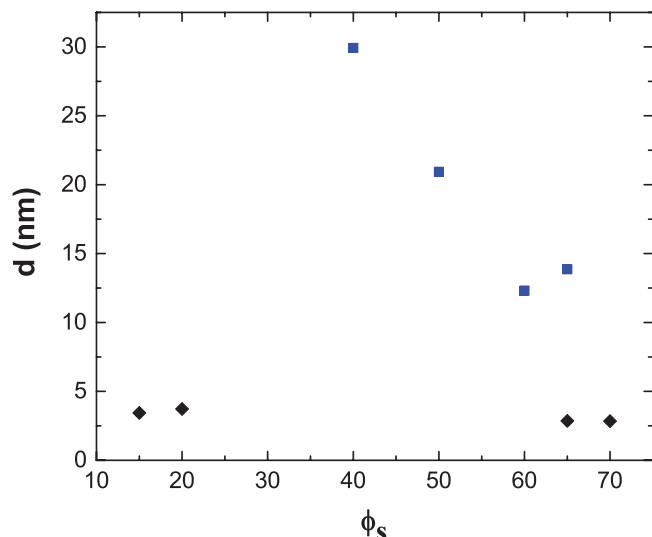
Figure 6. Characteristic length of DDAB-PAANa2100 complexes as a function of ϕ_s at $R = 14$. Periodicities (d) of the lamellar phases occurring at low and high ϕ_s are indicated by diamonds, and the average cell–cell distance (L) in the sponge phase by squares. For $20 < \phi_s < 40$, the value of L was not accessible with our SAXS system.
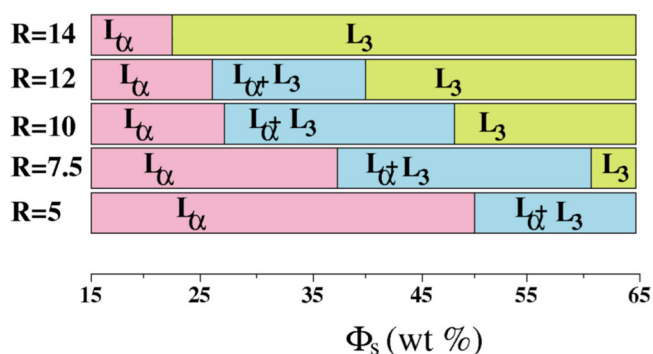

Figure 7. Partial phase diagram of DDAB-PAANa2100 complexes at 30 °C. The second collapsed phase occuring at $\phi_s > 65$ is not shown.

Figure 8. Lamellar periodicity of DDAB-PAANa8000 complexes as a function of ϕ_s at 30 °C and $R = 14$.

Figure 9. TGA traces of DDAB, PAANa, and DDAB-PAANa complexes at [NaBr] = 0 and 400 mM.

species makes it easier to determine their relative abundance in the complex. Three steps can be seen in the TGA curve of the low-c_s complex at around 100 °C, 200 °C and 400 °C. The step at 400 °C, corresponding to the polyelectrolyte, is absent in the TGA trace of the high-c_s complex. The composition of these complexes were also probed using CHN analysis. The C/N weight ratio of the high-c_s complex was found to be 23.4, which is very close to that obtained for the pure surfactant (23.8). On the other hand, the corresponding value for the low-c_s complex is 37.0, from which it can be estimated that the complex contains about 6 PAA monomers per surfactant molecule.

4. Discussion

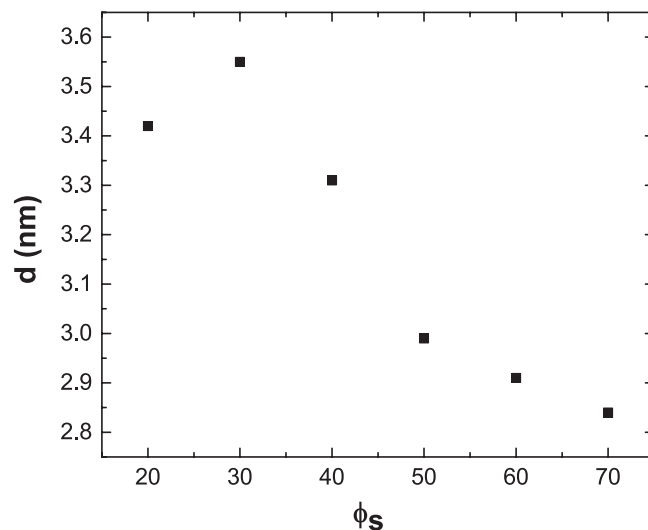Analogous to DDAC-PAANa complexes, DDAB-PAANa complexes exhibit a swelling transition followed by a de-swelling transition with increasing ϕ_s. As discussed in [5], the complex formation is accompanied by the release of the two counterions into the solution. Hence increasing ϕ_s increases the salt concentration, c_s, in the solution. Assuming that all the surfactant molecules are neutralized by the polyelectrolyte, which is in excess, c_s can be taken to be equal to the surfactant concentration in the solution. Increasing ϕ_s at fixed R increases both c_s as well as the concentration of uncomplexed polyelectrolyte in the solution, c_p. Figure 7 shows that both c_s and c_p play a role in the swelling transition, which occurs at higher values of c_s for lower values of c_p. The swelling and deswelling transitions also occur on increasing c_s at fixed c_p.

The polyelectrolyte adsorption layer formed at low c_s is heterogeneous as a result of inter-chain electrostatic repulsion

[6]. Hence it is reasonable to assume that the collapsed lamellar complex occurring at low c_s is stabilized by bridging of adjacent bilayers by the polyelectrolyte chains. Absence of the swelling transition for higher molecular weights of the polyelectrolyte, as seen in DDAC-PAANa complexes [5], can be attributed to the enhancement of the bridging attraction with increasing contour length of the polymer [7]. TGA and CHN analyses of the complexes clearly show that the low-c_s lamellar phase contains both the surfactant and the polyelectrolyte, whereas the high-c_s lamellar phase is composed of only the surfactant. This is in conformity with the reported inability of the polyelectrolyte chains to adsorb on the bilayer at high c_s, when the electrostatic attraction between the chains and the bilayer is fully screened [9]. This observation supports the hypothesis that the collapsed lamellar phase at high-c_s is stabilized by inter-bilayer van der Waals attraction. We have not studied the effect of the pH of the solution on the structure of the complexes. Since PAA is a weak polyelectrolyte, lowering the pH should affect its degree of dissociation. However, since the mass of a weak polyelectrolyte adsorbed on an oppositely charged surface shows an initial increase followed by a decrease with increasing salt concentration [6], we feel that the present observations will be qualitatively reproduced as long as the pH is not too low.

The only difference between DDAC-PAANa and DDAB-PAANa complexes is that the swollen phase occurring in the two systems at intermediate c_s have different structures. In the former it exhibits a lamellar phase, whereas the sponge (L_3) phase is found in the latter. Both these phases are made up of bilayers, but in the sponge phase it takes a highly convoluted morphology, leading to a bicontinuous partitioning of the bulk [19, 20]. As mentioned in the introduction, this swollen phase can in principle be stabilized by two types of repulsive interactions; steric repulsion between the adsorption layers and undulation repulsion between the polymer-adsorbed bilayers. In the case of steric repulsion, the maximum swelling will be decided by the thickness of the polymer layer, whereas it will depend on the value of κ in the case of undulation repulsion. In swollen complexes of DDAB-PAANa2100 as well as of DDAC-PAANa2100, the separation between the bilayers in the swollen phase is much longer than the contour length of the polymer [5]. Hence steric repulsion between the bilayers can be ruled out and one can attribute the large swelling of these complexes to undulation repulsion. In support of this proposal DDAC bilayers are found to exhibit an undulation stabilized lamellar phase, when the electrostatic inter-bilayer repulsion is screened out by salt, indicating a low value of κ [5]. From the structural similarity of DDAB and DDAC, DDAB bilayers can also be expected to have a low value of κ, which will allow them to swell in the presence of salt. As mentioned earlier, theoretical studies have shown that the L_α phase is stable over a narrow range of values of $\bar{\kappa}/\kappa$ centered around -1. For higher values of this ratio the L_3 phase is stable, whereas lower values favor vesicles [21, 22]. Polymer adsorption on a bilayer is expected to modify both κ and $\bar{\kappa}$ [15, 16]. κ is expected to decrease, whereas $\bar{\kappa}$ is expected to increase in the presence of an adsorption layer. Hence the

ratio $\bar{\kappa}/\kappa$ will increase in the presence of the adsorption layer, driving the $L\alpha$-L_3 transition. Experimental observations have been reported that are consistent with these predictions [26]. Although the above predictions are for the adsorption of neutral polymers on bilayers, the high salt concentration in the systems studied here make them relevant to the present case [27]. As discussed in [5], the large scatter in the lamellar periodicity of the swollen DDAC-PAANa complexes, which we attribute to the irreversible nature of the polymer adsorption process, makes it difficult to draw any conclusions regarding the effect of the adsorption layer on κ. This problem persists in the present system. However, formation of the sponge phase in the present system clearly shows that the presence of the adsorption layer increases the value of $\bar{\kappa}$.

Phase diagrams of the DDAC-water and DDAB-water systems are shown in supplementary material. The DDAC-water system exhibits the L_α phase over a very wide range of water content, stabilized by electrostatic inter-bilayer repulsion [28]. The DDAB-water system also forms the L_α phase over a broad concentration range, but there are some striking differences in their phase behaviour. The DDAB-water system is known to exhibit a metastable L_3 phase, which is absent in the DDAC-water system [1]. This suggests that DDAB bilayers have a higher value of $\bar{\kappa}$, close to the threshold value required to exhibit the L_3 phase. Another major difference between the two surfactant-water systems is the occurrence of a L_α−L_α transition in DDAB that is absent in DDAC. This behaviour is attributed to the presence of a strong short-range inter-bilayer attraction, arising from the tendency of Br$^-$ counterions to adsorb back on to the charged bilayers [2]. The coexistence region decreases with increasing temperature and disappears above a critical temperature. At higher temperatures an isotropic phase is found near this composition range, which is absent in the DDAC-water system [2]. The structure of this phase has not been probed in any detail, but it is known that the SAXS pattern of this phase shows a broad correlation peak as in the case of the L_3 phase. If this is indeed the L_3 phase, then it would be another indication that DDAB bilayers have a higher value of $\bar{\kappa}$, so that a smaller increase in $\bar{\kappa}$ is sufficient to push them into the L_3 phase compared to DDAC bilayers.

The reasons for the observed differences in the phase behavior of DDAC and DDAB bilayers remain poorly understood in spite of the relative simplicity of these systems [29]. Osmotic stress experiments have shown that the inter-bilayer interactions in these two systems are identical in the dilute regime and are dominated by electrostatic double layer repulsion [2]. However, in the intermediate concentration range, where DDAB bilayers exhibit the coexistence of two lamellar phases, interactions in these two systems differ significantly. In this case an additional non-electrostatic interaction that leads to the binding of the bromide ion to the bilayer has to be invoked in order to account for the observed behavior. A stronger attractive dispersion force between the bilayer and the highly polarizable bromide ion has been suggested as a possibility [2]. The relative propensity of DDAB bilayers to exhibit the sponge phase indicates that the binding of the bromide ion on the bilayer could also lead to changes in its elastic moduli.

5. Conclusion

We have studied the effect of an oppositely charged polyelectrolyte on the interaction between ionic surfactant bilayers, as a function of salt concentration in the solution. At low salt concentrations, polymer bridging between adjacent bilayers creates an effective inter-bilayer attraction, that results in a condensed lamellar complex. At high salt concentration the polyelectrolyte does not bind to the bilayers and the van der Waals inter-bilayer attraction leads to the formation of a collapsed lamellar phase. A swollen complex occurs over intermediate salt concentrations, which forms a bicontinuous sponge phase. Formation of the sponge phase can be attributed to an increase in the Gaussian rigidity of the bilayers due to polymer adsorption, as has been theoretically predicted.

ORCID iDs

V A Raghunathan ⬤ https://orcid.org/0000-0002-9213-1811

References

[1] Dubois M and Zemb T 1991 *Langmuir* **7** 1352
[2] Dubois M, Zemb T, Fuller N, Rand R P and Parsegian V A 1998 *J. Chem. Phys.* **108** 7855
[3] Israelachvili J N 2011 *Intermolecular and Surface Forces* 3rd edn (Amsterdam: Elsevier)
[4] Dahlgren M A G, Waltermo Å, Blomberg E, Claesson P M, Sjöström L, Åkesson T and Jönsson B 1993 *J. Phys. Chem.* **97** 11769
[5] Thomas M, Swamynathan K and Raghunathan V A 2019 *J. Chem. Phys.* **150** 094903
[6] Szilagyi I, Trefalt G, Tiraferri A, Maroni P and Borkovec M 2014 *Soft Matter* **10** 2479
[7] Podgornik R 1992 *J. Phys. Chem.* **96** 884
[8] Gradzielski M and Hoffmann I 2018 *Curr. Opin. Colloid Interface Sci.* **35** 124
[9] Xie F, Nylander T, Piculell L, Utsel S, Wågberg L, Åkesson T and Forsman J 2013 *Langmuir* **29** 12421
[10] Biggs S 1995 *Langmuir* **11** 156
[11] de Gennes P G 1982 *Macromolecules* **15** 492
[12] Helfrich W 1978 *Z. Naturforsch.* A **33** 305
[13] Helfrich W 1973 *Z. Naturforsch.* C **28** 693
[14] Chaikin P M and Lubensky T C 1995 *Principles of "Condensed Matter Physics* (Cambridge: Cambridge University Press)
[15] Brooks J T, Marques C M and Cates M E 1991 *J. Physique* II **1** 673
[16] Clement F and Joanny J F 1997 *J. Physique* II **7** 973
[17] Roux D and Safinya C R 1988 *J. Physique* **49** 307
[18] Dahlgren M A G 1994 *Langmuir* **10** 1580
[19] Porte G, Appell J, Bassereau P and Marignan J 1989 *J. Physique* **50** 1335
[20] Roux D, Coulon C and Cates M E 1992 *J. Phys. Chem.* **96** 4174
[21] Morse D C 1994 *Phys. Rev.* E **50** R2423
[22] Golubović L 1994 *Phys. Rev.* E **50** R2419
[23] Strey R, Jahn W, Porte G and Bassereau P 1990 *Langmuir* **6** 1635
[24] Pabst G, Rappolt M, Amenitsch H and Laggner P 2000 *Phys. Rev.* E **62** 4000
[25] Porcar L, Hamilton W A, Butler P D and Warr G G 2003 *Langmuir* **19** 10779
[26] Maugey M and Bellocq A M 2001 *Langmuir* **17** 6740
[27] Shafir A and Andelman D 2007 *Soft Matter* **3** 644
[28] Kang C and Khan A J 1993 *Coll. Int. Sci.* **156** 218
[29] Harries D, Podgornik R, Parsegian V A, Mar-Or E and Andelman D 2006 *J. Chem. Phys.* **124** 224702